Charge Symmetry Breaking in $np \to d\pi^0$

A. K. Opper,[1,*] E. Korkmaz,[2] D. A. Hutcheon,[3,4] R. Abegg,[3,4,†] C. A. Davis,[4,5] R. W. Finlay,[1] P. W. Green,[3,4] L. G. Greeniaus,[3,4] D. V. Jordan,[1,3,‡] J. A. Niskanen,[6] G. V. O'Rielly,[2,§] T. A. Porcelli,[2] S. D. Reitzner,[1,‖] P. L. Walden,[4,7] and S. Yen[4]

[1]*Ohio University, Athens, Ohio 45701, USA*
[2]*University of Northern British Columbia, Prince George, British Columbia, Canada*
[3]*University of Alberta, Edmonton, Alberta, Canada*
[4]*TRIUMF, Vancouver, British Columbia, Canada*
[5]*University of Manitoba, Winnipeg, Manitoba, Canada*
[6]*University of Helsinki, Helsinki, Finland*
[7]*University of British Columbia, Vancouver, British Columbia, Canada*

(Received 5 June 2003; published 21 November 2003)

The forward-backward asymmetry in $np \to d\pi^0$, which must be zero in the center-of-mass system if charge symmetry is respected, has been measured to be $[17.2 \pm 8.0(\text{stat}) \pm 5.5(\text{syst})] \times 10^{-4}$, at an incident neutron energy of 279.5 MeV. This observable is compared to recent chiral effective field theory calculations, with implications regarding the *du* quark mass difference.

DOI: 10.1103/PhysRevLett.91.212302 PACS numbers: 24.80.+y, 11.30.Er, 13.75.Cs, 25.10.+s

In the quark model, the breaking of charge independence and charge symmetry arises from the mass difference of the up and down current quarks and the electromagnetic interaction between quarks. The basic np interaction is particularly sensitive to such fundamental effects since the "background" Coulomb force is absent in this system. Indeed, charge symmetry breaking (CSB) has been unambiguously observed [1–3] in np elastic scattering at three different energies. Measurement of CSB in the inelastic $np \to d\pi^0$ reaction complements the existing data in that it is sensitive to contributions that are absent in the elastic channel, e.g., the exchange of an isospin mixed $\pi\eta$ meson. Furthermore, this reaction is unique as a testing ground for effective field theory calculations addressing the important issue of isospin symmetry violation in pion-nucleon scattering. The observable of interest in $np \to d\pi^0$ is the center-of-mass forward-backward asymmetry, A_{fb}, which we define as

$$A_{\text{fb}}(\theta) \equiv \frac{d\sigma(\theta) - d\sigma(\pi - \theta)}{d\sigma(\theta) + d\sigma(\pi - \theta)}, \tag{1}$$

where θ is the angle between the incident beam and the scattered deuteron. Note that the asymmetry must be zero if charge symmetry is conserved. We report on a measurement of this asymmetry at a neutron energy a few MeV above the reaction threshold (275.06 MeV) and compare our result to recent theoretical predictions [4,5] bearing on such fundamental questions as the *du* quark mass difference and our understanding of QCD dynamics and symmetries in low-energy hadronic interactions.

The experiment.—The experiment was performed at TRIUMF with a 279.5 MeV neutron beam, a liquid hydrogen target, and the SASP magnetic spectrometer [6] positioned at 0°. With these near threshold kinematics and the large acceptance of SASP, the full deuteron distribution from $np \to d\pi^0$ was detected in one setting of the spectrometer thereby eliminating many systematic uncertainties. These deuterons form a distinct kinematic locus in momentum versus laboratory scattering angle, which is shown in Fig. 1 for the collected data.

The TRIUMF CHARGEX facility [7] produced the neutron beam by passing a high intensity proton beam through a thin ^{7}Li target. A sweeping magnet deflected the primary proton beam into a well-shielded dump. The liquid hydrogen target (LH_2) was ~1 m downstream from the ^{7}Li target and contained within a flat cylindrical volume, with a nominal thickness of 2 cm. Two sets of veto counters (FEV1, FEV2) and a trigger counter set (FET) were each composed of a pair of plastic scintillators positioned above one another. This allowed more

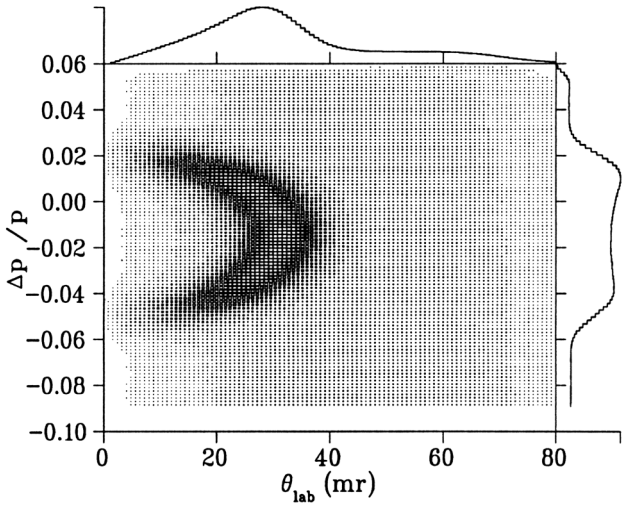

FIG. 1. Kinematic locus of $np \to d\pi^0$ data.

stable operation in the high (few MHz) particle rate environment. The thick veto scintillators were upstream of the LH_2 and shadowed it. The FET counters were positioned immediately downstream of the LH_2.

Three multiwire proportional chambers, positioned upstream of the SASP entrance (FECs, i.e., front-end chambers), provided tracking information for charged particles. Each FEC consisted of a pair of orthogonal wire planes. The first and last FECs were mounted to measure vertical and horizontal coordinates. The third FEC was positioned midway between the other two and rotated 40° with respect to them for efficiency measurements and to aid in multihit track reconstruction. Particle tracking near the SASP focal plane was provided by two vertical-drift chambers (VDCs). Three sets of scintillators, downstream from the VDCs, provided timing and particle identification information as well as sufficient redundancy to determine the efficiencies of all focal plane area detectors.

Measurements of np elastic scattering with incident neutron beams that filled the same target space and produced protons that spanned the momentum distribution of the $np \to d\pi^0$ reaction provided a stringent test of the description of the spectrometer acceptance. Further details on the apparatus and other technical aspects of the measurement are found in Ref. [8].

Extraction of $A_{\rm fb}$.—Close to threshold, the $np \to d\pi^0$ cross section in the center-of-mass frame is given by

$$\frac{d\sigma}{d\Omega}(\theta) = A_0 + A_1 P_1(\cos\theta) + A_2 P_2(\cos\theta), \qquad (2)$$

where P_1 and P_2 are Legendre polynomials. The A_0 and A_2 coefficients were previously measured [9] at a number of energies within 10 MeV above threshold. The presence of charge symmetry breaking is reflected in the A_1 term as it is odd in $\cos\theta$. In this standard parametrization, the angle integrated form of $A_{\rm fb}$ is given by $A_{\rm fb} = \frac{1}{2} A_1/A_0$.

For a given beam energy, $\cos\theta$ varies linearly with the longitudinal component of deuteron momentum in the laboratory reference frame. Ideally, the $\cos\theta$ distribution would be found by a suitable, simple projection of the data of Fig. 1. However, the measured deuteron locus is distorted by energy loss, multiple scattering, energy spread of the beam, and spectrometer acceptance making a direct extraction of $A_{\rm fb}$ impossible. Instead, the data were binned according to laboratory momentum and angle (as in Fig. 1) and compared to a model which represented the background due to $C(n, d)$ reactions as a low-order polynomial and generated the locus of $H(n, d)\pi^0$ events by Monte Carlo simulation of the beam, target, reaction cross section, spectrometer, and detectors. Empty target data helped constrain the description of the background.

The simulation was based on GEANT3. It began with a proton beam incident on the ^{7}Li target and included energy loss by the proton beam as well as the angular and energy distribution of neutrons from the $^7\mathrm{Li}(p, n)$ reaction. Production of deuterons according to the distribution of Eq. (2) was allowed in the LH_2 target and other hydrogenous material such as scintillators and their wrapping. Standard GEANT tracking options were adopted for deuteron energy loss and multiple scattering but the reaction losses, which amount to 1%–2% and are momentum dependent, were parametrized from data on deuteron elastic and reaction cross sections from hydrogen and carbon [10]. Tracking through the SASP dipole used a field map obtained at 875 A and scaled up to the operating current of 905 A. Data were acquired in ten different periods spanning two years and the simulation accounted for measured detector efficiencies, scintillator thresholds, missing FEC wires, and known changes in target thickness in a manner consistent with the actual running periods.

To reduce the possibility of psychological bias in matching simulation to data, a blind analysis technique was used which incorporated a hidden offset to the A_1/A_0 asymmetry parameter of the $np \to d\pi^0$ generator. The collaborators developing the simulation and extracting the observable did not know the value of the offset until all consistency checks had been satisfied.

Systematic effects.—The acceptance of SASP is a function of the initial target position and direction of the deuteron as well as its momentum. Nonuniformities in the momentum acceptance of SASP would systematically produce a false asymmetry and had to be limited. High-statistics data from np elastic scattering were collected and compared to model simulations to determine a fiducial volume of uniform acceptance. For these calibration measurements, the SASP magnets were set to their values for the $np \to d\pi^0$ running, but the primary beam energy was adjusted so that the elastically scattered protons had a momentum deviation $\delta = (p - p_0)/p_0 = -4, 0$ or $+4\%$ compared to the central momentum of the deuterons of interest. The momentum range of those deuterons was approximately $\pm 3.5\%$. Projections of the np elastic data direction for position slices were formed, and the ratios of yields at -4% vs $+4\%$ were formed for both data and simulation; see Fig. 2. The analysis software acceptance cuts in position and direction were then limited to the regions common to both data and simulation which were uniform in momentum to the statistical precision of the data. The flatness of the distributions with full acceptance cuts (Figs. 2(c) and 2(d)) illustrates the uniformity in momentum.

Simulation versus simulation comparisons were carried out to determine how strongly experimental parameters and other effects were correlated with A_1/A_0. For example, momentum dependent deuteron reaction losses and detection efficiencies are obvious mechanisms which can mimic the effect of a nonzero A_1/A_0. Combining each correlation with the independently determined uncertainty of its parameter gave the systematic contributions shown in Table I. However, for the LH_2 target

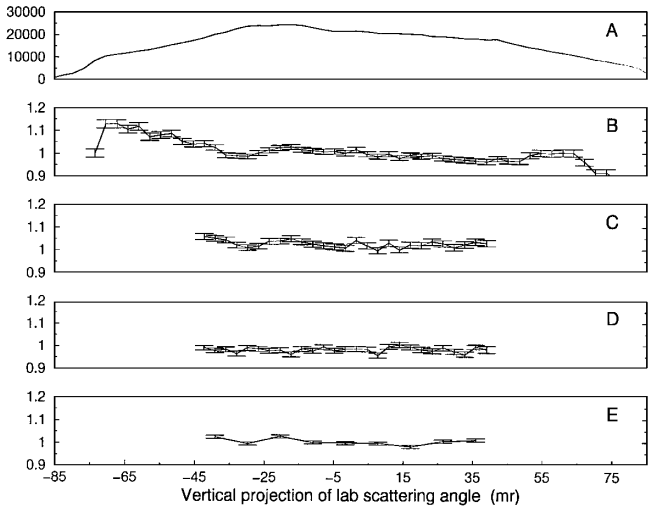

FIG. 2. The vertical projection of the lab scattering angle for the center acceptance slice, elastic np scattering; (a) data yield for $\delta = -4\%$, no cuts; (b) data ratio ($-4\%/+4\%$), no cuts; (c) data ratio ($-4\%/+4\%$), full acceptance cuts; (d) simulation ratio ($-4\%/+4\%$), full acceptance cuts; (e) ratio of (c) to (d), normalized to the center bin.

thickness, the proton beam energy (T_{beam}), and the central momentum of SASP (p_0), the independent information was not a sufficient constraint. Therefore, these three parameters, along with A_1/A_0, were treated as free parameters and their values extracted from fitting the data. To this end, simulations were made and χ^2 calculated for 81 points in a four-dimensional space, in which each of the four free parameters was stepped above and below a nominal value. χ^2 minimization techniques [11] were then used to obtain the values of the parameters relative to nominal values, at the global χ^2 minimum, while the local curvature of the χ^2 surface gave their errors and mutual correlations.

As a test of the model, the χ^2 calculations and fitting were repeated on subsets of the data and simulated data, selected according to whether the reaction occurred in the top or bottom part of the LH_2 target. A second test divided events into those originating in the left or right part of the target. The best fit values and errors of A_1/A_0 (after removal of the offset) and the other three parameters are presented in Table II.

The root mean square (rms) systematic error for the full acceptance and the four subspaces is $\sim 2.7\%$ in a rectangular binning scheme of 50 bins in δ and 20 bins in θ, indicating a substantial discrepancy between data and the simulation. Pixel by pixel examination of the contribution to χ^2 revealed a systematic difference in the profile of the locus along lines of steepest ascent. The sign of the differences tended to be positive at the peak and negative at both the "inner" and "outer" margins of the locus, possibly due to inadequate treatment of deuteron scattering in the simulation.

A change in A_1/A_0 will not change the ratio of counts in peak versus margins of the locus because it multiplies $\cos(\theta_{\text{cm}})$. In contrast, the LH_2 thickness, p_0, and T_{beam} all shift or broaden the locus and thus are sensitive to the ratio of locus counts at the peak versus margins. It is reasonable to expect further rebinning to remove sensitivity to unimportant details of the simulation without losing sensitivity to A_1/A_0. We repeated the χ^2 grid search using 20 bins in δ and 10 bins in θ, and again with 10 bins in δ and 5 bins in θ. As expected, the fractional error dropped to 2.1% and 1.4%, respectively, with A_1/A_0 remaining consistent within errors. A more sophisticated binning scheme which treated the locus as a set of "elliptical" and "radial" bins on top of rectangular background bins produced an rms error of 2.1% for 2500 background bins and 36 locus bins, and an rms error of 1.2% for 100 background bins and 6 locus bins. In all fits and binning schemes the best fit values of the asymmetry in the acceptance subspaces agreed within errors with the value for the full acceptance, which is $(34.4 \pm 16) \times 10^{-4}$, implying $A_{\text{fb}} = [17.2 \pm 8.0(\text{stat}) \pm 5.5(\text{syst})] \times 10^{-4}$.

Theoretical predictions of A_{fb} have been made by Niskanen [4] using a meson-exchange coupled-channel model which showed that the major contribution by far is due to $\pi\eta$ (and $\pi\eta'$) mixing in both the exchange and produced (outgoing) mesons. At our energy the prediction is $A_{\text{fb}} = -28 \times 10^{-4}$, when accepted values are used for the ηNN coupling constant and the $\pi^0\eta$ mixing matrix

TABLE I. Systematic error contributions to A_{fb}.

	Uncertainty $\times(10^{-4})$
FEV threshold	2.5
Separation between front and rear FECs	2.5
Longitudinal position of ^{7}Li	2.5
A_2/A_0	2.0
Deuteron reaction losses	1.5
Detection efficiencies	1.5
Primary beam energy spread	1.0
Neutron angle	1.0
Background	1.0
FET threshold	0.5
Total	5.5

TABLE II. Stability of the four free parameters over target subspaces; b = bottom; t = top; l = left; r = right.

	(A_1/A_0) (10^{-4})	Relative LH_2 (mm)	Relative p_0 (MeV/c)	Relative T_{beam} (MeV)
Full	34.4 ± 16	0.94 ± 0.05	0.365 ± 0.015	0.048 ± 0.001
b	30 ± 26	0.39 ± 0.09	0.547 ± 0.025	0.086 ± 0.002
t	20 ± 20	1.14 ± 0.07	0.236 ± 0.018	0.021 ± 0.002
l	29 ± 23	1.21 ± 0.08	0.273 ± 0.021	0.042 ± 0.002
r	15 ± 22	0.75 ± 0.08	0.427 ± 0.021	0.051 ± 0.002

element ($g^2_{\eta NN}/4\pi = 3.68$ from meson-exchange NN potential models [12] and $\langle\pi^0|\mathcal{H}|\eta\rangle = -0.0059\ \mathrm{GeV}^2$ from analysis of η decay data [13]). More recently, A_{fb} was revisited [5] within the framework of chiral effective field theory where the issue of charge symmetry breaking in the rescattering amplitude of the exchanged pion was addressed. The resulting additional contribution to A_{fb} is then expressed in terms of two parameters δm_N and $\overline{\delta} m_N$ representing contributions from the *du* quark mass difference and from electromagnetic effects within the nucleon, respectively. Specifically, at our energy, A_{fb} is expressed as

$$A_{\mathrm{fb}} = -0.28\%\left[\left(\frac{g_{\eta NN}}{\sqrt{4\pi(3.68)}}\right)\left(\frac{\langle\pi^0|\mathcal{H}|\eta\rangle}{-0.0059\ \mathrm{GeV}^2}\right) - \frac{0.87}{\mathrm{MeV}}\left(\delta m_N - \frac{\overline{\delta} m_N}{2}\right)\right], \quad (3)$$

where the first term arises from $\pi\eta$ mixing and the second from $\pi^0 N$ scattering. With the introduction of the new term, A_{fb} changes sign and becomes positive with an estimated upper value around $+69 \times 10^{-4}$, when large but reasonable values of δm_N and $\overline{\delta} m_N$ are used [5]. Our positive experimental result strongly suggests, therefore, that such isospin violating $\pi^0 N$ interactions as outlined in Ref. [5] are indeed significant.

The parameters δm_N and $\overline{\delta} m_N$ are also constrained by the neutron-proton mass difference as

$$\Delta_N = m_n - m_p = \delta m_N + \overline{\delta} m_N = 1.29\ \mathrm{MeV}. \quad (4)$$

When our A_{fb} result is combined with Eqs. (3) and (4), and the values given above for the ηNN coupling constant and $\pi\eta$ mixing matrix element, we find that $\delta m_N = 1.66 \pm 0.27$ MeV and $\overline{\delta} m_N = -0.36 \pm 0.27$ MeV, assuming no uncertainties in the $\pi\eta$ mixing term or in the theoretical model. Although our value of $\overline{\delta} m_N$ agrees with that of Gasser and Leutwyler [14] (i.e., -0.76 ± 0.30 MeV), we emphasize that this last exercise is only meant to illustrate the significance and potential important implications of our A_{fb} result. Further theoretical studies are currently underway [15] to accommodate simultaneously the new CSB result of our study and that of a recent cross-section measurement of the isospin forbidden reaction $dd \rightarrow \alpha\pi^0$ [16].

This work was supported by grants from The Natural Sciences and Engineering Research Council of Canada, The National Science Foundation, and The Ohio Supercomputer Center. TRIUMF is operated under a grant from the National Research Council of Canada.

*Email address: opper@ohiou.edu
†Deceased.
‡Current address: Pacific Northwest National Labs, Richland, WA 99352, USA.
§Current address: University of Massachusetts, Dartmouth, North Dartmouth, MA 02747, USA.
‖Current address: The Ohio State University, Columbus, OH 43210, USA.

[1] R. Abegg *et al.*, Phys. Rev. Lett. **56**, 2571 (1986); Phys. Rev. D **39**, 2464 (1989).
[2] R. Abegg *et al.*, Phys. Rev. Lett. **75**, 1711 (1995).
[3] L. D. Knutson *et al.*, Phys. Rev. Lett. **66**, 1410 (1991); S. E. Vigdor *et al.*, Phys. Rev. C **46**, 410 (1992).
[4] J. A. Niskanen, Few-Body Syst. **26**, 214 (1999).
[5] U. van Kolck, J. A. Niskanen, and G. A. Miller, Phys. Lett. B **493**, 65 (2000).
[6] P. L. Walden *et al.*, Nucl. Instrum. Methods Phys. Res., Sect. A **421**, 142 (1999).
[7] R. Helmer *et al.*, Can. J. Phys. **65**, 588 (1987).
[8] D. A. Hutcheon *et al.*, Nucl. Instrum. Methods Phys. Res., Sect. A **459**, 448 (2001).
[9] D. A. Hutcheon *et al.*, Nucl. Phys. **A535**, 618 (1991).
[10] A. Auce *et al.*, Phys. Rev. C **53**, 2919 (1987); H. Okamura *et al.*, Phys. Rev. C **58**, 2180 (1998); C. Baumer *et al.*, Phys. Rev. C **63**, 037601 (2001).
[11] W. Press, S. Teukolsky, W. Vetterling, and B. Flannery, *Numerical Recipes* (Cambridge University Press, Melbourne, 1992).
[12] O. Dumbrajs *et al.*, Nucl. Phys. **B216**, 277 (1983).
[13] S. A. Coon *et al.*, Phys. Rev. D **34**, 2784 (1986).
[14] J. Gasser and H. Leutwyler, Phys. Rep. **87**, 77 (1982).
[15] A. C. Fonseca, A. Gardestig, C. Hanhart, C. J. Horowitz, G. Miller, J. A. Niskanen, A. Nogga, and U. van Kolk (private commuunication).
[16] E. J. Stephenson *et al.*, Phys. Rev. Lett. **91**, 142302 (2003).